Received: 27 July 2023 | Revised: 10 January 2024 | Accepted: 20 January 2024
DOI: 10.37917/ijeee.21.2.1 Vol. 21 | Issue 2 | December 2025

Open Access

Iraqi Journal for Electrical and Electronic Engineering
Original Article

A Litz Wire-Based Inductor Model for a DC-DC Converter-Fed Single-Phase Inverter

S. Ramesh*[1], K. Karunanithi[1], G. Thirumurugan[1], S. P. Raja[2]
[1]Department of Electrical and Electronics Engineering, Vel Tech Rangarajan Dr.Sagunthala R&D Institute of Science and Technology, Chennai, India
[2]School of Computer Science and Engineering, Vellore Institute of Technology, Vellore, Tamilnadu, India

Correspondance
*S. Ramesh
Department of EEE, Vel Tech Rangarajan Dr.Sagunthala R&D Institute of Science and Technology, Chennai, Tamilnadu, India
Email: rameshsme@gmail.com

Abstract
Inductors play a major role in the power electronics domain, particularly in DC-DC converter design. The objective of this paper is to reach inductance value by means of fewer turns, using Litz wire wound on a ferrite core. In the manufacture of inductors, the key aspects of the design criteria include the choice of the core material, the type of copper coil and insulation materials, and their overall size. Taking into consideration the design parameters with no compromises on performance, Litz wire with the least turns is introduced into an inductor in certain DC-DC converters. Once the DC settled voltage is reached, it is given to a single-phase inverter for loading and application measures. This approach provides a small-level inductor design for maximized efficiency with improved thermal behavior. The hardware model for the proposed method has been developed using a DC-DC converter fed with a single-phase inverter model. The proposed DC-DC converter has been tested, performance-wise, by applying different load levels. It is observed, from the results, that the Litz wire-based approach achieves maximum efficiency with improved thermal behavior.

Keywords
DC-DC Converter, Ferrite Core, Litz Wire, Single-Phase Inverter, Thermal Behaviour.

I. Introduction

The goal of the hardware design and electronic manufacturing service sectors is to reduce the size, weight and manufacturing time of power electronic products. The domains of electronics and magnetics are closely linked. The use of Litz wire, which is made up of thin insulated wires woven or twisted to spread the current density over its large cross-sectional regions, enhances the performance of high frequency (HF) magnetic modules. The name "Litz wire" comes from the German word, "litzendraht," which means "woven wire".

Litz wire has uses in heat exchangers, electrical drives, on-board charging of electric cars and wireless charging of EVs and mobile devices in the automobile industry. Inverters and solar energy-powered motors use HF Litz wire, which has wide-ranging applications in industrial manufacture, including antennas, detectors, motors, pumps and inverters, as well as supply lines and strings. They also have applications in industrial kitchens, for example, in electric cooking ovens or ceramic heaters. Litz wire is widely used in medicine, across a range of instruments and applications, including listening assistance systems as well as high frequency cables and external coils in magnetic resonance imaging systems. Furthermore, coils constructed from enameled wire and Litz wire are used in smartphone wireless chargers.

Litz wire is considered an equivalent replacement for the standard copper wire mostly used in induction heating applications. This model in this study enhances the overall efficiency and power consumption while reducing losses and size [1]. At resonance voltages, inductance value drops drastically, owing to which well-designed inductors are indispensable to proper heating. This major factor is addressed by the thermal properties of the different materials involved in inductor construction, chiefly the Litz wire in the flow path [2]. The proximity effect must be mitigated for medium frequency inductors and transformers to function effectively. High frequency multi-stranded conductors that deploy Litz cable are commonly used to resolve this problem because the cable allows for low distortion and retains stability in the magnetic model [3]. To prevent losses caused by adjoining spaces infringing on certain areas, high frequency wires are used. If the radius of the shielded strands is less than the skin depth, the skin effect may be ignored and uniform current sharing can be maintained [4]. The litz wire helps to maintain the winding resistance even when high air gap fringing fields are approaching towards the winding [5]. Induction cookers work best on 15 kHz when induction Litz wire winding is used. A comparison of Litz wire and solid wire shows that the former is clearly superior [6]. This is because linear current flow through standard wires, stranded, twisted, and Litz wire is generally considered to have lower AC resistance than solid wire. The use of Litz wire significantly reduces thermal rise [7]. Litz wire air-cooled coils minimize power loss and simplify the water cooling setup process [8].

Magnetic components are essential for power converters, and contribute significantly to the system's scale, failure, and expense. Their design, however, is usually complex and time-consuming, owing to the number of turns involved. The high current and low current windings that are difficult to manufacture raise costs, take up extra room size, and increase leakage inductance [9], [10]. The appropriate magnetic material is needed for a small and cost-effective inductor. Material with scattered air gaps, high saturation flux, and relatively low power loss both within the winding and core is desirable [11–14].

Based on the discussions above, Litz wire is chosen in this paper to help build an inductor model with a DC-DC converter-fed single-phase inverter. This paper has addressed the importance and advantages of Litz wire over standard copper coil in Section 1. In Section 2, the key design aspects of inductor manufacture are dealt with. Section 3 describes the experimental setup of the DC-DC converter connected to a single-phase inverter. Section 4 analyses the performance of the proposed Litz wire-based DC-DC converter at different input voltage levels, and Section 5 concludes the paper.

II. The Proposed Inductor Design

Materials selection is a key component of inductor construction. The core of an inductor is made up of a variety of materials of varying B-H curves. Eddy current losses cause the core temperature to rise, particularly when high frequencies are used in the converter. The temperature of the inductor is affected by convective and radiative convection.

The temperature of a prototype of the desired inductor should be determined when it works at the rated values. If the temperature is unusually hot or cold, the design is to be adjusted. In the proposed design, a ferrite core and Litz wire are used to obtain the required inductance value. Ferrite core is predominantly selected for economical design and to minimize eddy current flow [5]. The detailed design procedure for litz wire is given in Fig.1.

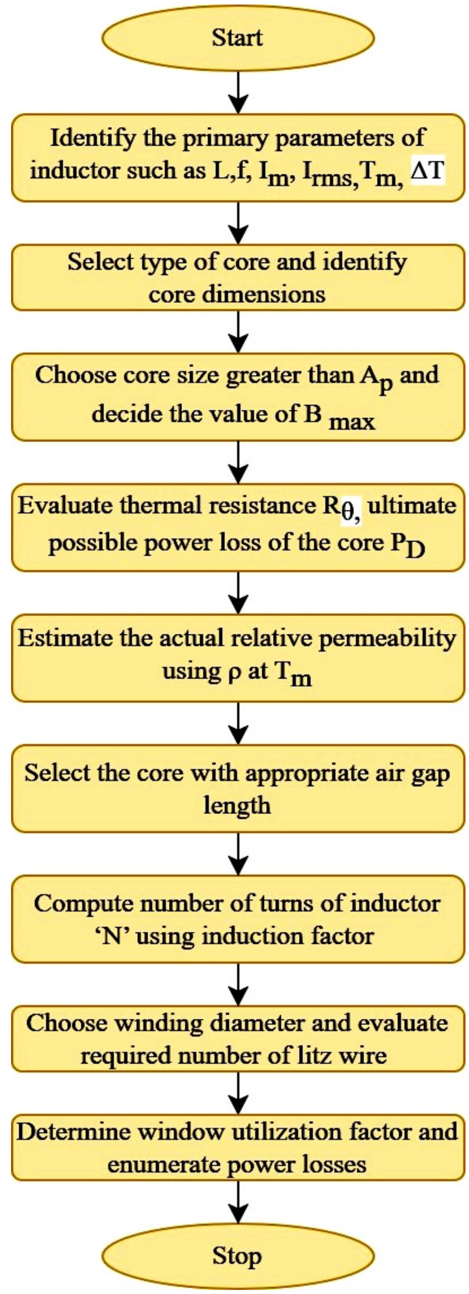

Fig. 1. Flow Chart.

Figure 2 illustrates the proposed Litz wire-based inductor model wound on a ferrite core covered with insulation. The details of the inductor core model are represented in Table I and the number of layers with its specifications are illustrated in Table II.

TABLE I.
CORE DETAILS.

Parameter	Details of parts
Core manufacture	Ferro x cube
Core material	Ferrite
Type of core	ETD49

Fig. 2. A Litz wire-based inductor as a transformer model.

TABLE II.
LAYER DETAILS.

Layers	Parameter	Value
Layer 1	Thickness	250-350 μm
	Insulation type	2 turns of NOMEX
Layer 2	No.of turns	16 Turns-350 μH
	Wire OD – 5.2 mm	AWG4 Round Litz wire
	Wire length	120cm
Layer 3	Thickness	250-350 μm
	Insulation type	2 turns of NOMEX
Layer 4	No.of turns	4 Turns
	Wire OD–2.5mm	AWG10 Round Litz wire
	Wire length	30cm

The optimum value of litz inductor already designed by [5, 15, 16] and it is expressed by the following equation

$$L_{opt} \approx C f_s^{\frac{\alpha-\beta}{2+\beta}} - \frac{V_o}{4 f_s I_{DC}} \tag{1}$$

Where,
f_s – Switching frequency in Hz
α, β – steinmetz parameters – 1.30, 2.59 respectively.
V_o – Output Voltage in V
I_{DC} – DC component of current in A

The core size of the litz wire is evaluated by the following expression (2)

$$A_p = \left(\frac{K_i L I_{max}^2}{K_t B_{max}} \sqrt{\frac{7(1+\gamma)}{9 k_u \Delta T}} \right)^{\frac{8}{7}} \tag{2}$$

The required number of litz wire is given by following equation (3)

$$\eta_{Litz} = \frac{K_i I_{max}}{7 J_o A_{Strand}} \tag{3}$$

The ferrite core loss is given by [17] the following equation (4)

$$P_{fe} = \frac{N_1}{N_2} P_m = \frac{1}{T_s} \int_0^{T_s} i_p(t) N_1 \frac{dB(t)}{dt}\, dt \tag{4}$$

Where,
P_{fe} – Ferrite core losses in W
N_1 – Number of turns in primary side
N_2 – Number of turns in secondary side
P_m – Measured power in W
I_p – RMS current of the primary winding in A
$B(t)$ – Instantaneous flux density in T

III. EXPERIMENTAL SETUP OF THE DC-DC CONVERTER

The most popular systems for adjusting voltage levels in DC-DC applications are boost and buck converters. Energy is passed from input to output by means of an inductor in these converters, with respect to increased or decreased or constant voltage levels. Both the boost and buck conversion techniques are fully effective only if the active and passive components of the entire circuit are lossless. Furthermore, by changing the duty cycle of the active switch through a continuous regulation of the output voltage, maximum efficiency can be achieved. The critical component of magnetics greatly impacts efficiency. The proposed approach attempts to break barriers in the development of inductors and reach maximum efficiency.

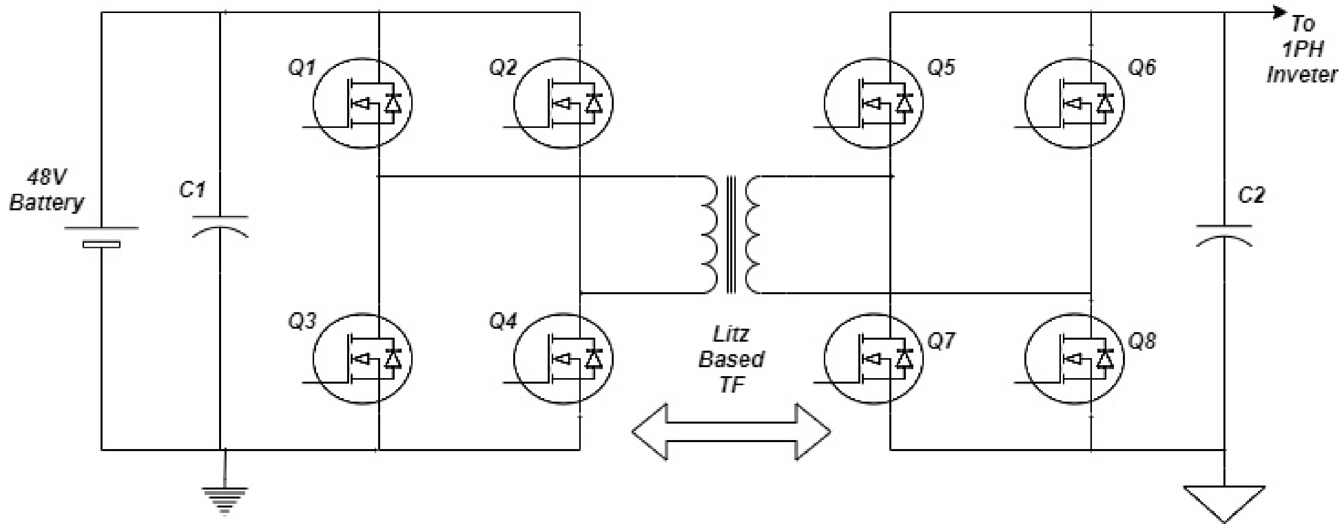

Fig. 3. Full bridge DC-DC converter with the proposed magnetics.

TABLE III.
DC-DC CONVERTER COMPONENT DETAILS.

Parameter/ Component	**Value/ Quantity**	**Part Number**
Power rating	2000W	DC-DC converter
Input voltage	38-52 V	Rectifier
Intermediate voltage	$400V_{dc}$	DC-DC converter
Load	1 Phase inverter	R, RL Load
MOSFET	4	ST 9220E
MOSFET	4	AOT92S
Magnetics	1	Proposed inductor
Capacitor	1	2200 μF/80V
Capacitor	1	180 μF/450V

For the experimental verification, a full bridge DC-DC converter is selected, and its circuit layout shown in Fig. 3. The layout comprises four MOSFETs, driven sinusoidally by a high frequency Litz wire-wound inductor. Further, the MOSFETs are used for rectification, with capacitor filters added where necessary for pure DC voltage. The components and their values are mentioned in Table III. The gate pulses are generated using a microcontroller and driver circuits to ensure that the switches function perfectly at every stage. To avoid high switching losses in MOSFET and to diminish losses in Litz inductor, a common operating frequency of 100 kHz is selected [3]. Waveform patterns are followed, in line with the basic concept of the full bridge DC-DC converter, as shown in Fig. 4.

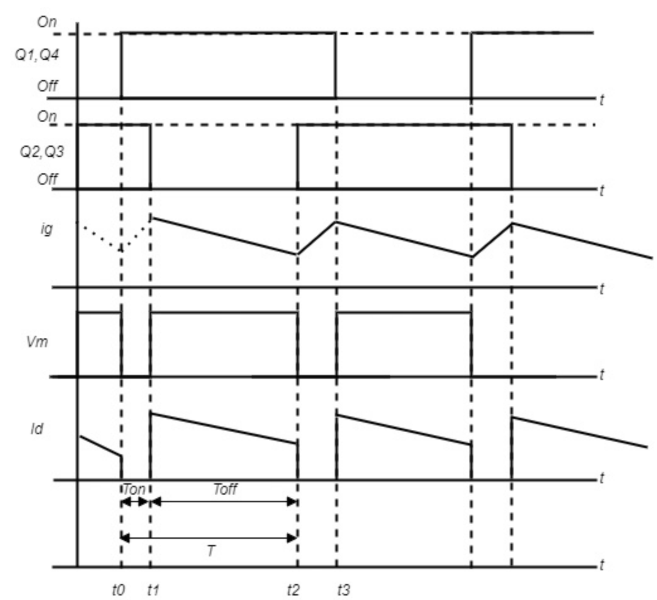

Fig. 4. Waveforms for the DC-DC converter.

A. Synchronous Rectification

It is commonly known that a MOSFET structure comprises an inherent body diode in parallel; hence, a complete bridge can only be built utilizing four MOSFETs. The voltage across a conventional diode varies from 0.6V to 1.0V, based on the current running through it and the technology driving the diode, which is the primary source of power loss in the bridge. The setup of simply employing the body diode of a MOSFET appears to be much worse. If the MOSFET is powered via synchronous rectification, the body diode links only for a very brief duration of the waveform matching the dead times of the regulated MOSFETs. The regulated MOSFETs are driven into conduction for the majority of the sinusoidal current input. The waveforms and applied pulses are shown in Fig.5.

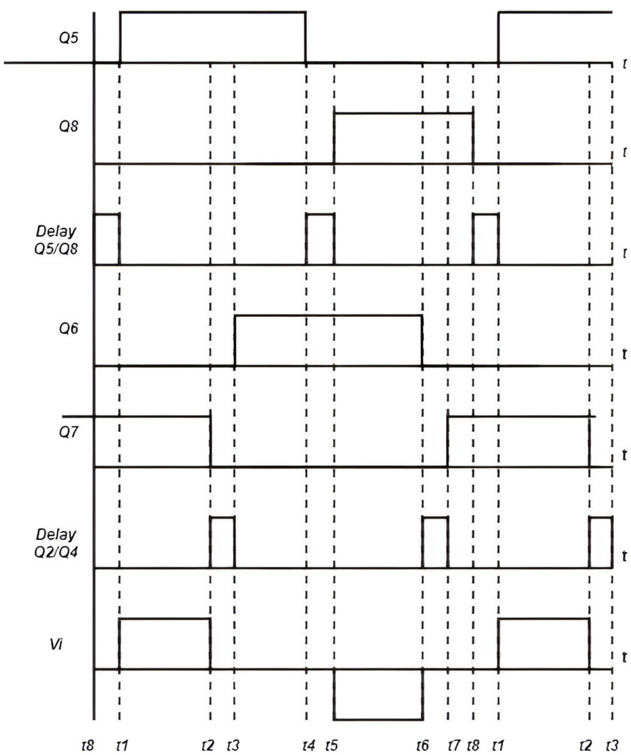

Fig. 5. Waveforms for the synchronous rectifier.

B. Single-phase inverter

A majority of appliances and loads function on sinusoidal voltage. An inverter is a circuit that transforms DC voltage into AC voltage at the required output level and frequency. A 230V, 50Hz single phase inverter is selected to test and validate the efficiency of the converter. Figures 6 and 7 illustrate the circuit diagram and appropriate waveforms of the single-phase inverter model.

C. LC Filter Design

The output of a single phase two pulse inverter will be square waveform as shown in Fig. 7. To utilize the inverter output for any loading applications, the output voltage and current will be in sinusoidal form. To convert the square waveform into sinusoidal waveform and to reduce the output ripples, a simple LC filter circuit is essential [18].

Since the LC filter design procedure for the single-phase full bridge inverter is discussed in [18], the nearest practical values of L and C are utilized in this research. Table IV specifies the details of the components used in the inverter model.

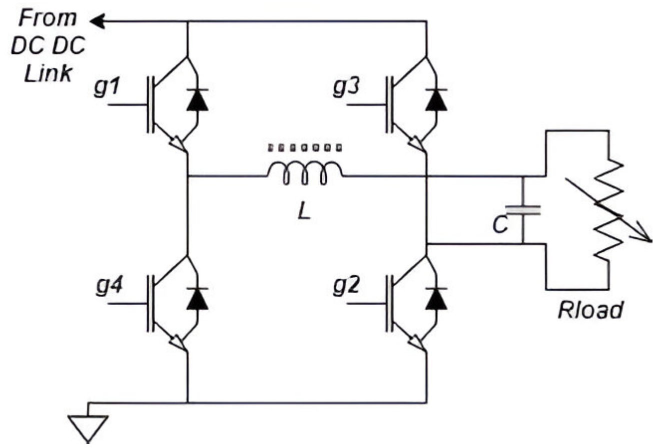

Fig. 6. Single-phase inverter.

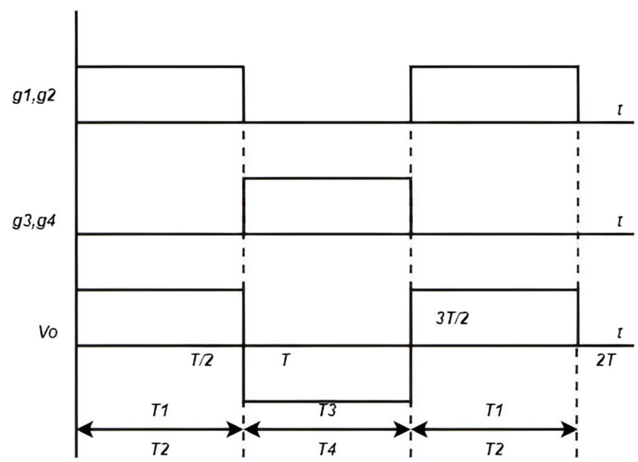

Fig. 7. Waveforms of the gate pulses and output voltage.

TABLE IV.
DC-AC INVERTER COMPONENT DETAILS.

Parameter/ Component	Value/ Quantity	Part Number
Power Rating	2500W-1 no.	Inverter
IGBT	4	IRF1010
L Filter [18]	1	100 μH
C Filter [19]	1	2.35 μF
R Load	200-2000W	-
L Load	1 μH to 100mH	-

IV. Experimental Study

The proposed Litz wire-based inductor model is successfully implemented to operate a single-phase resistive load application with a maximum power requirement of 2500W in a laboratory environment. The hardware implementation of the proposed model is shown in Fig. 8 and Fig. 9. Two different input voltage levels are considered in order to study the performance of the converter, which is designed for a 48V DC operating voltage. The performance of the converter is studied with respect to the rated 48V DC and the reduced input supply voltage of 40V as well.

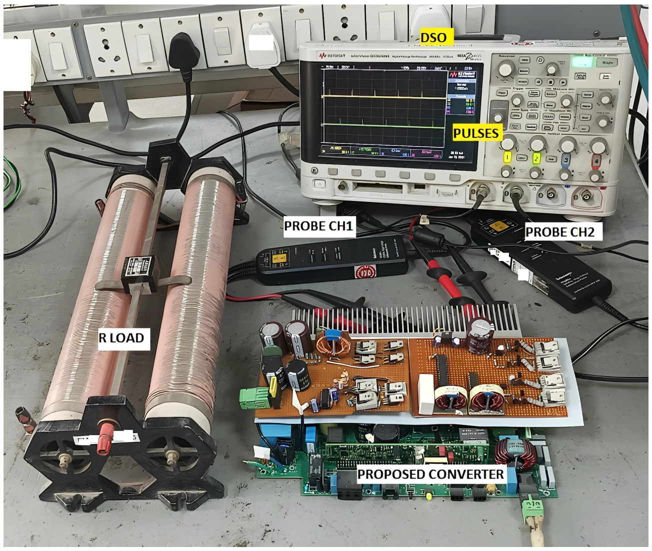

Fig. 8. Hardware implementation of the proposed converter.

Fig. 9. Hardware implementation of the proposed system with R-L load

A. *Input 48V-Output 230V/50Hz Efficiency*

Table V indicates the converter DC voltage, current and power, respectively, if the input voltage of 48V is given to a single-phase resistive load. For increased load values ranging from 28 W to 2373 W, the experimental readings are reported for the converter and inverter voltage, current and power values. It is observed that the maximum efficiency (η) of 95.78% occurs at 1399 W of output power for the proposed Litz-based inductor in the experimental study.

TABLE V.
Readings of Hardware model for 48V input DC voltage with R Load.

V_{dc}	I_{dc}	P_{dc}	$V_{ac}out$	$I_{ac}out$	$P_{ac}out$	η
49.23	0.57	28.06	234.66	0.00	0.00	0.00
49.13	4.56	224.03	231.84	0.86	198.90	88.78
49.09	9.01	442.30	231.83	1.73	400.00	90.44
48.98	13.51	661.72	231.78	2.64	612.90	92.62
48.88	17.68	864.20	231.34	3.45	798.90	92.44
48.77	21.90	1068.06	230.87	4.32	996.90	93.34
48.66	26.34	1281.70	230.81	5.19	1197.10	93.40
48.54	30.09	1460.57	230.84	6.06	1399.00	95.78
48.44	35.27	1708.48	230.70	6.91	1594.00	93.30
48.32	39.90	1927.97	230.80	7.78	1795.00	93.10
48.19	44.72	2155.06	230.69	8.69	2003.00	92.94
48.06	49.39	2373.68	230.52	9.52	2195.00	92.47

B. *Input 40V-Output 230V/50Hz Efficiency*

The experimental study has been extended further to include a drop in input voltage levels while the same load power requirements continue to be met. It is observed from the results reported in Table VI the overall efficiency is still maintained at above 90%.

TABLE VI.
Readings of Hardware model for 40V DC voltage with R load.

V_{dc}	I_{dc}	P_{dc}	$V_{ac}out$	$I_{ac}out$	$P_{ac}out$	η
42.03	0.66	27.74	234.78	0.00	0.00	0.00
41.91	5.57	233.44	231.81	0.86	198.70	85.12
41.80	10.63	444.33	231.76	1.72	399.30	89.86
41.68	15.99	666.46	231.86	2.64	613.20	92.01
41.57	20.73	861.75	231.41	3.45	799.30	92.75
41.43	25.91	1073.45	230.93	4.32	996.80	92.86
41.30	31.11	1284.84	230.90	5.19	1197.60	93.21
41.22	36.59	1508.24	230.90	6.06	1399.00	92.76
41.06	41.98	1723.70	230.95	6.92	1598.00	92.71
40.92	47.34	1937.15	230.73	7.78	1795.00	92.66
40.68	53.37	2171.09	230.73	8.69	2004.00	92.30
40.54	58.99	2391.45	230.65	9.53	2198.00	91.91

Using the R load at the output terminal varying from 200W to 2000W, maximum efficiency at 95.78 is noted, using the Litz-based inductor in the experimental setup and study.

C. Proposed system under RL Load

Most of the practical applications entails with RL load. To validate the performance of the system more efficiently, a variable inductor is added in series with the rheostat load. The value of R and L increased gradually to examine the performance. The proposed system is experimented with RL load under 48V and 40V are measured and tabulated in Table VII and Table VIII respectively.

TABLE VII.
READINGS OF HARDWARE MODEL FOR 48V INPUT DC VOLTAGE WITH RL LOAD.

V_{dc}	I_{dc}	P_{dc}	$V_{ac}out$	$I_{ac}out$	$P_{ac}out$	η
49.23	0.57	28.06	234.66	0.00	0.00	0.00
49.11	4.52	221.98	231.67	0.84	194.60	87.67
49.05	8.95	439.00	231.59	1.68	389.07	88.63
48.91	13.42	656.37	231.48	2.54	587.96	89.58
48.83	17.59	858.92	231.37	3.40	786.66	91.59
48.72	21.82	1063.07	230.65	4.25	980.26	92.21
48.59	26.24	1275.00	230.45	5.16	1189.12	93.26
48.48	30.07	1457.79	230.42	5.96	1373.30	94.20
48.36	35.22	1703.24	230.33	6.85	1577.76	92.63
48.27	39.84	1923.08	230.12	7.64	1758.12	91.42
48.14	44.63	2148.49	229.79	8.52	1957.81	91.13
48.05	49.33	2370.31	229.64	9.39	2156.32	90.97

TABLE VIII.
READINGS OF HARDWARE MODEL FOR 40V DC VOLTAGE WITH RL LOAD.

V_{dc}	I_{dc}	P_{dc}	$V_{ac}out$	$I_{ac}out$	$P_{ac}out$	η
42.03	0.66	27.74	234.78	0.00	0.00	0.00
41.85	5.54	231.85	231.67	0.85	196.92	84.93
41.72	10.46	436.39	231.45	1.67	386.52	88.57
41.59	15.91	661.70	231.31	2.59	599.09	90.54
41.45	20.67	856.77	231.25	3.4	786.25	91.77
41.38	25.87	1070.50	230.82	4.28	987.91	92.28
41.27	31.08	1282.67	230.63	5.13	1183.13	92.24
41.15	36.57	1504.86	230.54	5.98	1378.63	91.61
40.98	41.9	1717.06	230.42	6.79	1564.55	91.12
40.85	47.21	1928.53	230.07	7.62	1753.13	90.91
40.57	53.21	2158.73	229.85	8.5	1953.73	90.50
40.45	58.75	2376.44	229.53	9.32	2139.22	90.02

Fig. 10 represents the relationship between increased power levels and overall efficiency at rated 48V. It is noticed that the efficiency is retained at above 90% even for the high-power requirements of a resistive load or RL load. Similarly, Fig. 11 indicates the power and efficiency curve at 40V. From Figures 10 and 11, it is observed that the efficiency of the system is almost equal during R or RL loading conditions. The performance of the proposed system is examined with a suitable RL load. The output voltage and current waveforms are measured and illustrated in Fig.12 for RL load. From the output waveforms, it is observed that there is a small deviation in voltage and frequency due to the increase in RL load.

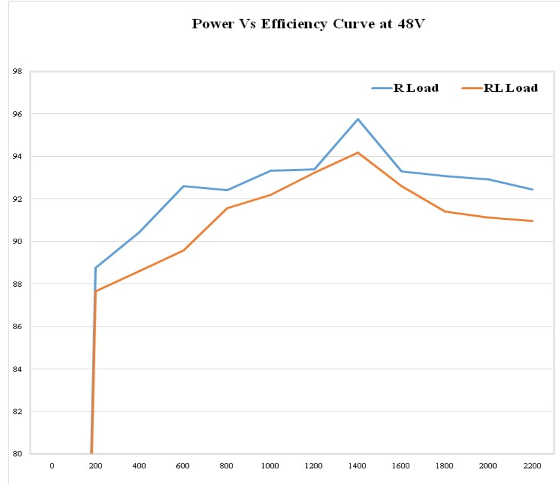

Fig. 10. Power Vs Efficiency at a rated voltage of 48V.

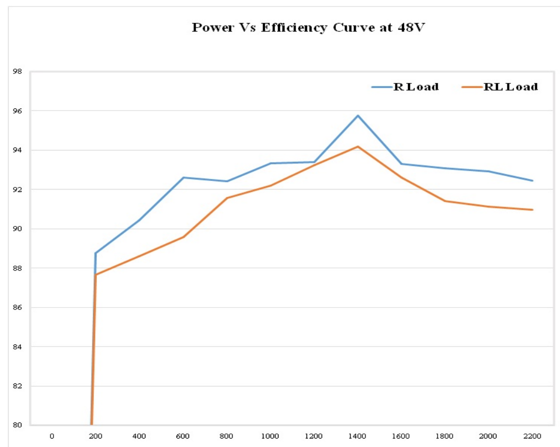

Fig. 11. Power Vs Efficiency at 40V DC voltage.

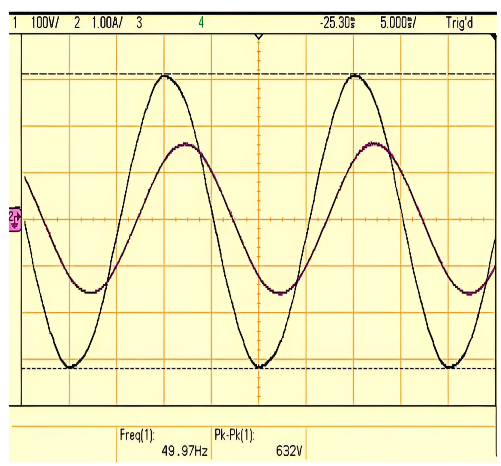

Fig. 12. Output waveform with RL load.

V. Conclusion

This paper has addressed the design of inductor winding using Litz wire, having considered the advantages and disadvantages of selected wires. The insulation products available and their application-based capabilities have been discussed. An attempt has been made to design a perfect inductor with a small number of turns for a power electronic-based system application. Using an experimental prototype setup, the performance of the converter is verified after considering the relevant input data. The purpose of the DC-DC converter and single-phase inverter is to validate the performance of the inductor in every aspect. The experimental results have shown that the proposed DC-DC converter-fed single-phase inverter model contributes significantly lesser weight and dimensions than the normal inductor-based design. It is hoped that converter designers will use this method to circumvent complex and sophisticated optimization strategies.

Acknowledgment

The authors are thankful to the AICTE for creating modern power electronics facility under MODROBS scheme to the Department of Electrical and Electronics Engineering, Vel Tech Rangarajan Dr. Sagunthala R&D Institute of Science and Technology. The First and corresponding author is grateful to the Management for supporting this research through Institute-funded Seed Money.

Conflict of Interest

The authors have no conflict of relevant interest to this article.

References

[1] C. Roth and D. Gerling, “Novel calculation model for bunched litz wires,” *2019 IEEE Wireless Power Transfer Conference (WPTC)*, pp. 162–165, 2019.

[2] D. Barth, B. Klaus, and T. Leibfried, “Litz wire design for wireless power transfer in electric vehicles,” *2017 IEEE Wireless Power Transfer Conference (WPTC)*, pp. 1–4, 2017.

[3] S. Ehrlich, H. Rossmanith, M. Sauer, C. Joffe, and M. März, “Fast numerical power loss calculation for high-frequency litz wires,” *IEEE Transactions on Power Electronics*, vol. 36, no. 2, pp. 2018–2032, 2021.

[4] A. K. Paul, “Current density characterization of litz wires used in induction heating coils: A practical approach,” *2018 IEEE International Conference on Power Electronics, Drives and Energy Systems (PEDES)*, pp. 1–6, 2018.

[5] P. Papamanolis, T. Guillod, F. Krismer, and J. W. Kolar, “Minimum loss operation and optimal design of high-frequency inductors for defined core and litz wire,” *IEEE Open Journal of Power Electronics*, vol. 1, pp. 469–487, 2020.

[6] A. Reatti and F. Grasso, “Solid and litz-wire winding non-linear resistance comparison,” *Proceedings of the 43rd IEEE Midwest Symposium on Circuits and Systems (Cat.No.CH37144)*, vol. 1, pp. 466–469, 2000.

[7] A. S. Kaittan, “Comparison study between solid and litz wires of induction cooker,” *2018 1st International Scientific Conference of Engineering Sciences - 3rd Scientific Conference of Engineering Science (ISCES)*, pp. 86–91, 2018.

[8] J. Schutz, J. Roudet, and A. Schellmanns, “Modeling litz wire windings,” *IAS ’97. Conference Record of the 1997 IEEE Industry Applications Conference Thirty-Second IAS Annual Meeting*, vol. 2, pp. 1190–1195, 1997.

[9] C. Alvarez, M. Bellaredj, and M. Swaminathan, “Open and closed loop inductors for high-efficiency system-on-package integrated voltage regulators,” *2019 IEEE 69th Electronic Components and Technology Conference (ECTC)*, pp. 1672–1679, 2019.

[10] A. Stadler, “The optimization of high frequency inductors with litz-wire windings,” *2013 International Conference-Workshop Compatibility And Power Electronics*, pp. 209–213, 2013.

[11] T. Guillod, J. Huber, F. Krismer, and J. W. Kolar, “Litz wire losses: Effects of twisting imperfections,” *2017 IEEE 18th Workshop on Control and Modeling for Power Electronics (COMPEL)*, vol. 34, pp. 1–8, 2017.

[12] M. Delhommais, J. Schanen, F. Wurtz, C. Rigaud, S. Chardon, and S. Vighetti, “Thermal model of litz wire toroidal inductor based on experimental measurements,” *2018 IEEE Applied Power Electronics Conference and Exposition (APEC)*, pp. 2658–2665, 2018.

[13] R. Y. Zhang, J. K. White, J. G. Kassakian, and C. R. Sullivan, “Realistic litz wire characterization using fast numerical simulations,” *2014 IEEE Applied Power Electronics Conference and Exposition - APEC 2014*, pp. 738–745, 2014.

[14] X. Li, Y. Zhang, J. Liu, and P. Zeng, “High step-up dc-dc converter based on multi-cell coupled inductor diode-capacitor network,” *2018 International Power Electronics Conference (IPEC-Niigata 2018 -ECCE Asia)*, pp. 2646–2652, 2018.

[15] M. Ngo, Y. Cao, D. Dong, and R. Burgos, "Design of 500 khz, 18 kw low leakage inductance intraleaved litz wire transformer for bi-directional resonant dc-dc converter," *IEEE Applied Power Electronics Conference and Exposition (APEC)*, p. 1153–1161, 2021.

[16] C.-T. Phan-Tan, T. Ngo-Phi, and N. Nguyen-Quang, "Design procedure and implementation of inductor using litz wires for induction heating," *2023 International Conference on System Science and Engineering (ICSSE)*, p. 370–374, 2023.

[17] S. Somkun, T. Sato, V. Chunkag, A. Pannawan, P. Nunocha, and T. Suriwong, "Performance comparison of ferrite and nanocrystalline cores for medium-frequency transformer of dual active bridge dc-dc converter," *Energies*, vol. 14, no. 9, p. 2407, 2021.

[18] A. Khoshkbar-Sadigh, V. Dargahi, K. Lakhera, and K. Corzine, "Analytical design of lc filter inductance for two-level inverters based on maximum ripple current," *IECON 2019 - 45th Annual Conference of the IEEE Industrial Electronics Society*, p. 1621–1626, 2019.

[19] P. A. Kyaw, M. Delhommais, J. Qiu, C. R. Sullivan, J.-L. Schanen, and C. Rigaud, "Thermal modeling of inductor and transformer windings including litz wire," *EEE Transactions on Power Electronics*, vol. 35, no. 1, p. 867–881.